Acta metall. mater. Vol. 41, No. 3, pp. 685–692, 1993
Printed in Great Britain.

0956-7151/93 $6.00 + 0.00

MATERIAL RESPONSE UNDER STATIC AND SLIDING INDENTATION LOADS

S. J. SHARP, M. F. ASHBY and N. A. FLECK
Cambridge University Engineering Department, Trumpington St, Cambridge CB2 1PZ, England

(Received 28 September 1992)

Abstract—Material response to indentation loads can be elastic, plastic, brittle (cracking), or various combinations of these. The details of the stress state in the material beneath the indenter depend on the material response and on whether the indenter is static or slides: when it slides, frictional tractions modify the field. In this paper, we map material properties on axes which allow the dominant response to indentation loads to be identified, for static and sliding indenters.

1. INTRODUCTION

Indentation loads appear in engineering structures when components touch, are clamped together, impact, or slide while pressed into contact (Fig. 1). The response of the material can be elastic (a rubber O-ring seal, for instance), or plastic (the usual response in a conventional hardness test) or brittle (impact on glass), or it can be combinations of these, of which elastic–plastic response is the most important. The sliding case differs from the other three because of friction, which introduces tangential or shearing tractions at the contact surface in addition to the normal tractions caused directly by the indentation force.

Indentation response cannot be inferred directly from known tensile response: materials which are brittle in tension can be plastic when indented. This is because the material response depends on stress state as well as on the intrinsic properties of the material. The stress state under a static indenter differs from that in a tensile test and both differ from that under a sliding indenter with friction.

In this paper we develop a simple scheme to reveal the response of a wide range of materials under three modes of loading: simple tension, static indentation and sliding indentation. We seek to span the widest possible range of material properties. The diagrams which follow contain, at one extreme, elastomers and foamed polymers and, at the other extreme, diamond.

2. THE METHOD

Material response to load can be elastic, plastic or brittle. Equations can be developed for the load required, in any given mode of loading, to cause a specified deformation of each of these possible mechanisms. That requiring the lowest load is taken to be dominant. Many simplifications are implicit in this assumption; among them, that the load increases monotonically (so that a material element has not, at an earlier time, seen higher loads nor is subject to fatigue conditions). It wil become apparent that the wide range of axes justify making these simplifying assumptions. The method will first be illustrated by

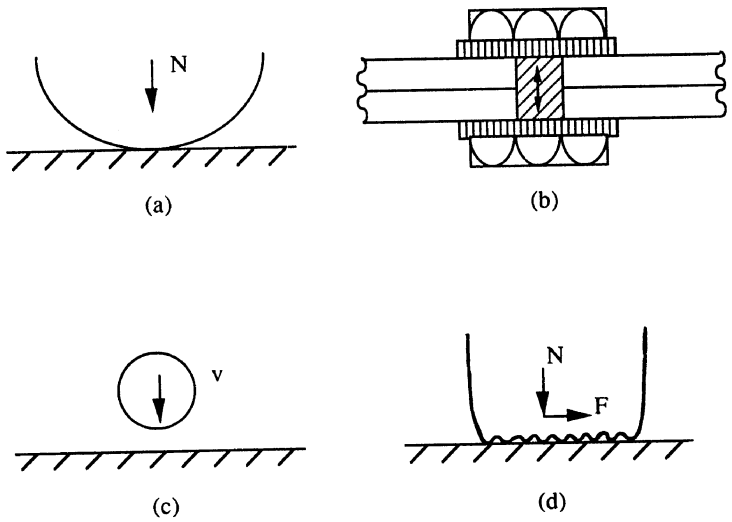

Fig. 1. (a) Static indentation, (b) clamping, (c) impact, (d) sliding with normal load and friction.

Table 1. Symbols, definitions and units

F	Indentation force (N)
R	Ball radius (mm)
a	Contact radius (mm)
E	Young's modulus (GPa)
σ_y	Yield strength (MPa)
k	Shear yield strength (MPa)
J_{1C}	Mode I toughness, tear energy etc. (kJ/m^2)
c	Flaw size (μm)
ν	Poisson's ratio

applying it to simple tensile loading; the more complicated cases involving indentation then follow. The same scheme can be applied to other stress states (compression, or torsion for instance) if required.

The method has features in common with that developed by Johnson [1]. One difference is the method of presentation: the axes of our diagrams contain material properties only and are thus independent (at the level of approximation used here) of the geometry and loading; these factors are introduced by overlaying further information on the figures.

2.1. *Simple tensions*

A cylindrical sample of a material, loaded in tension at low temperature (such that it does not creep) may deform elastically, it may yield plastically, or it may fracture in a brittle manner (Fig. 2). An elastic extensional strain ϵ requires a stress

$$\sigma = E\epsilon \quad \text{(elastic)} \tag{1}$$

where E is Young's modulus.

Plasticity occurs if the stress exceeds the yield strength

$$\sigma \geqslant \sigma_y \quad \text{(plastic)}. \tag{2}$$

Finally, if the material contains incipient cracks of length c, it will fail by brittle fracture if

$$\sigma \geqslant \frac{K_{1C}}{\sqrt{\pi c}} = \left(\frac{EJ_{1C}}{\pi c}\right)^{1/2} \quad \text{(brittle)}. \tag{3}$$

Here, K_{1C} is the fracture toughness and J_{1C} is the toughness or tear energy. (The formulation with J_{1C} rather than K_{1C} is preferred here because of the very wide range of materials and test methods with which we deal.) Consider attempting to apply a given elastic extension ϵ to the material. Its response will, in fact, be elastic only if the stress defined by equation (1) is less than that of equations (2) and (3); if it is not, the material will yield or fracture before the elastic strain ϵ is reached. Materials for which

$$E\epsilon \leqslant \sigma_y$$

and

$$E\epsilon \leqslant \left(\frac{J_{1C}}{\pi c}\right)^{1/2} \tag{4}$$

will remain elastic, all others will not. These two relations define (with the equality signs) boundaries which separate materials which are elastic at a strain ϵ from those which are not. Combining equations (2) and (3) defines, in a similar way, a plastic/brittle boundary. The elastic/plastic boundary is expressed as

$$\frac{\sigma_y}{E} = \epsilon; \tag{5}$$

the elastic/brittle boundary as

$$\left(\frac{J_{1C}}{E}\right)^{1/2} = \epsilon(\pi c)^{1/2}; \tag{6}$$

the plastic/brittle boundary as

$$\frac{\left(\frac{J_{1C}}{E}\right)^{1/2}}{\left(\frac{\sigma_y}{E}\right)} = (\pi c)^{1/2}. \tag{7}$$

Written in this way, it becomes clear that two, not three, material properties are involved: they are σ_y/E and J_{1C}/E. The first is dimensionless; the second has the dimensions of length.

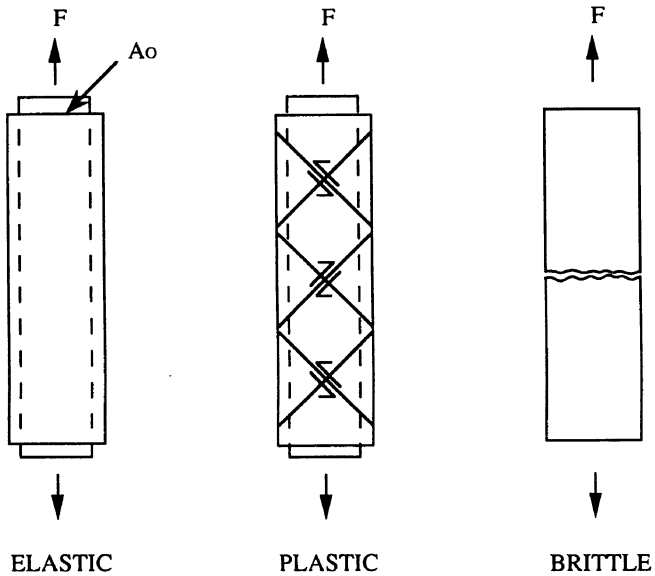

Fig. 2. Material response in tension can be elastic, plastic or brittle.

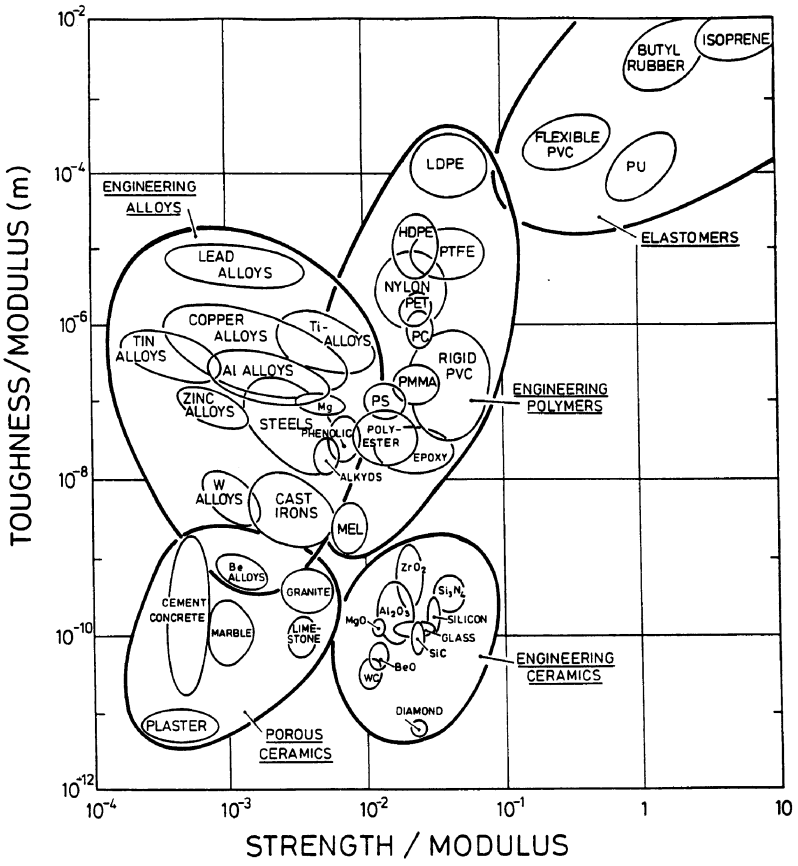

Fig. 3. A materials selection chart showing toughness/modulus (J_{IC}/E) plotted against yield strength/modulus (σ_y/E).

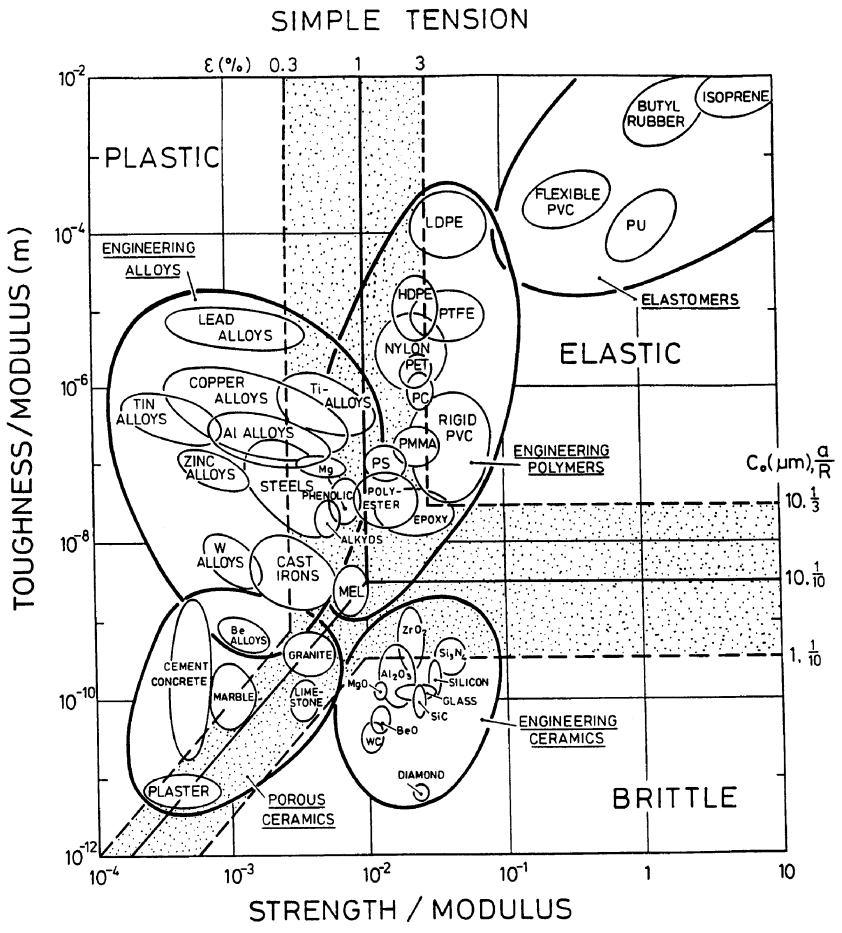

Fig. 4. The chart of Fig. 3, showing the mechanism–transition boundaries for simple tension.

This suggests the idea of displaying materials on axes of these two quantities. Figure 3 shows the result: it is a form of "materials selection chart" [2–4]. The axes are logarithmic and cover a range wide enough to include almost all materials: metals, ceramics, polymers, elastomers, foams and so on. A material appears as an ellipse which spans the range of its properties. Materials of a given class (metals, for instance) cluster together and are enclosed in heavy outline.

The figure allows the response of materials to various sorts of loading to be explored. Figure 4 shows the response to tensile loads. The boundaries between the elastic, plastic and brittle regimes are described within their range of applicability by equations (5)–(7). The solid boundaries are constructed for a strain $\epsilon = 1\%$ and an incipient crack length, c of 10 μm. The broken lines shows the effect of changing these; the corresponding values of ϵ and c are given on the figure. As expected, at an imposed strain of 1%, ceramics lie in the brittle field; most metals lie in the plastic field and polymers and elastomers lie in the elastic field. Increasing the strain to 3% moves the more brittle polymers into the brittle field and expands the plastic field to include the more ductile polymers.

All this is as expected. The power of the method appears when other stress states are examined. Even under complicated loading patterns, like that produced by indentation, the material response at the simplest level is captured by the properties σ_y/E and J_{1C}/E. The new stress state simply shifts the boundaries of the three regimes and can introduce a fourth: that of elastic–plastic, or contained–plastic response. The following sections illustrate this.

2.2. *Static indentation*

A spherical indenter of radius R, is pressed by a force F onto the flat surface of the material (Fig. 5). If the indenter and the material have the same modulus E and Poisson's ratio ν and the response is elastic, the contact radius a is related to the force F by

$$F = \frac{2}{3R}\frac{a^3E}{(1-\nu^2)} \tag{8}$$

[1]. (If the indenter modulus is much greater than that of the surface being indented this increases a slightly, by the factor $2^{1/3}$.)

If the peak stress beneath the indenter just exceeds the yield strength, the contact ceases to be perfectly elastic and becomes, instead, elastic–plastic. The first onset of plasticity occurs at a mean indentation pressure approximately equal to the yield stress [5, part I, p. 13], that is at a force F given by

$$F = 2\pi a^2 k = \pi a^2 \sigma_y \tag{9}$$

where $k \approx \sigma_y/2$ is the shear-yield strength. In this regime the plastic strains are of the same order as the surrounding elastic strains. As the load is increased, the plastic zone grows. When it breaks out to the surface, the contact becomess fully plastic and the plastic strains become much larger than the elastic strains. Within the fully plastic regime, the mean indentation pressure is approximately three times the yield stress [5]. This gives the relationship between force F and indent size a as

$$F = 3\pi a^2 \sigma_y. \tag{10}$$

It is helpful to have an approximate expression linking F and a between these two limits. Samuels and Mulhearn [6] point out that displacements produced by a blunt indenter are approximately radial from the point of first contact and that contours of equal strain form a set of approximately hemispherical surfaces. Then, using a Tresca yield criterion, Johnson [1] shows that

$$F \approx \tfrac{2}{3}\pi a^2\left[2 + \ln\left(\frac{Ea}{3\sigma_y R}\right)\right]\sigma_y. \tag{11}$$

When the yield strength of the material is high and the fracture stress low, the Hertzian (elastic) field beneath the indenter may reach the fracture stress before the yield stress is exceeded anywhere. Lawn and Wilshaw [7] equate the peak tensile stress associated with the elastic field to the fracture stress of equation (3) to give, in our terminology

$$F = \frac{6\pi a^2 (EJ_{1C})^{1/2}}{\sqrt{\pi c}}. \tag{12}$$

Equations (8)–(12) are used to define the boundaries of the regimes, much as equations (1)–(3) were used in the last section. Consider applying a force to a spherical indenter, pressing it into the test material, with the aim of creating a contact of chosen radius a. An elastic contact of this size can be produced only if the force defined by equation (8) is less than that

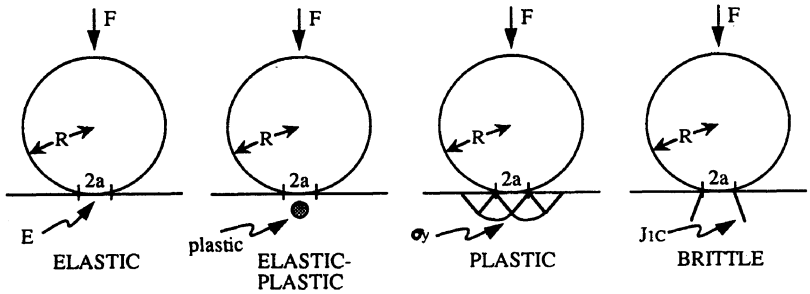

Fig. 5. Material response in static contact may be elastic, elastic–plastic, plastic or brittle.

of equations (9)–(12). The boundary of the elastic regime is found by equating (8) to each of the others in turn. The response is brittle in the regime in which (12) is less than (8)–(11), defining the brittle boundary, and so on. The equations for these boundaries are as follows.

The elastic/elastic–plastic boundary is given by

$$\frac{\sigma_y}{E} = \frac{2a}{3\pi R(1-\nu^2)}. \tag{13}$$

The elastic–plastic/fully plastic boundary is

$$\frac{\sigma_y}{E} = \frac{a}{3R}\exp\left(-\frac{5}{2}\right). \tag{14}$$

The fully-plastic/fully plastic boundary is

$$\frac{\sigma_y}{E} = \frac{2}{\sqrt{\pi c}}\left(\frac{J_{1C}}{E}\right)^{1/2}. \tag{15}$$

The elastic/brittle boundary is

$$\left(\frac{J_{1C}}{E}\right)^{1/2} = \frac{2}{9\pi}\frac{a}{R}\sqrt{\pi c}. \tag{16}$$

Finally, the elastic–plastic/brittle boundary is

$$\frac{\sigma_y}{E} = \frac{9}{\sqrt{\pi c}\left[2+\ln\left(\frac{Ea}{3\sigma_y R}\right)\right]}\left(\frac{J_{1C}}{E}\right)^{1/2}. \tag{17}$$

The boundaries are plotted in Fig. 6. As strain is proportional to a/R the solid boundaries are for chosen values of $a/R = 0.1$ and $c = 10\,\mu$m (in the same way that those in Fig. 5 were for $\epsilon = 1\%$ and $c = 10\,\mu$m). The broken lines show how the boundaries move for other values of a/R and c.

A comparison of Figs 4 and 6 shows that under indentation conditions the elastic field expands relative to the plastic and brittle fields, because plastic constraints and the largely compressive nature of the field inhibit plasticity and fracture. The figures identify the materials, which under each mode of loading, fall into each of the fields and the way in which non-material parameters (ϵ, a/R, c) influence this.

2.3. Indentation with sliding

A spherical indenter of radius R is pressed by a force F onto the flat surface of the material, and is made to slide across the surface by a tangential force, T, where

$$T = \mu F$$

and μ is the coefficient of friction (Fig. 7). For simplicity we assume (as before) that the indenter and material have the same moduli E and Poisson's ratio ν. When $\mu > 0$, the stress field beneath the indenter is changed and regimes of elastic, plastic and brittle response are displaced. We calculate their new position

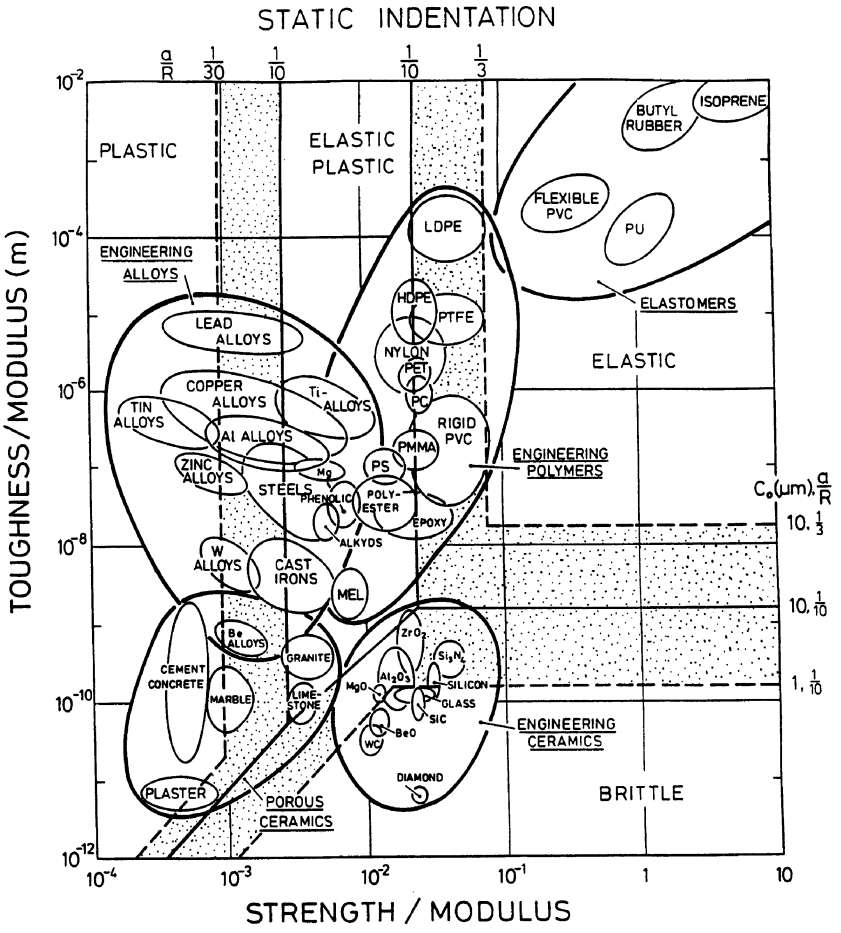

Fig. 6. The chart of Fig. 3, showing the mechanism–transition boundaries for static indentation.

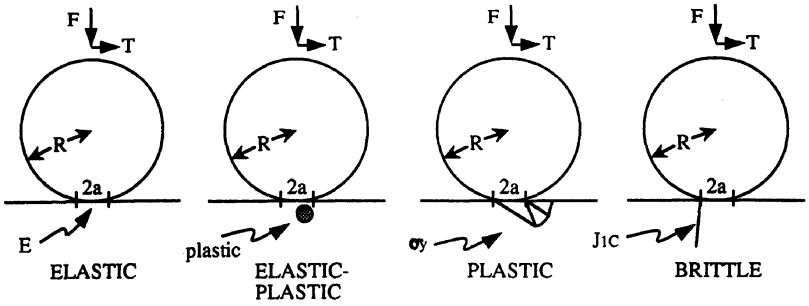

Fig. 7. Material response in sliding contact may be elastic, elastic–plastic, plastic or brittle.

for a "typical" value of $\mu = 0.5$; the calculation is easily repeated for other values.

The size of an elastic contact remains unchanged when a tangential force is added. The relation between the force F and the contact radius a is still given by equation (8). Brittle behaviour beneath a sliding contact has been the subject of numerous studies [8–10]. A recent attempt to pull these results together [11], using the results of Hamilton [12], leads to a result with the form of earlier equations in this paper for the force F at which fracture initiates from an initial surface flaw of length c. For $\nu = 1/3$ it reduces to

$$F = \frac{\pi a^2}{1.12[\frac{1}{6} + \frac{13}{16}\pi\mu]}\left(\frac{EJ_{1C}}{\pi c}\right)^{1/2}. \tag{18}$$

When $\mu = 0.5$, this force is about 1/10 of that given by equation (12) for static indentation.

The plastic response is a little more difficult. As μ increases, the point of first yield, based on a Von Mises criterion, moves towards the surface; yield first occurs at the surface when $\mu \geqslant 0.3$. Johnson [1, p. 208] shows how the contact pressure $F/\pi a^2$ for the first yield falls as μ increases. For present purposes the response is adequately approximated by

$$F = \frac{\pi a^2 \sigma_y}{\sqrt{1 + \alpha\mu^2}} \tag{19}$$

where $\alpha = 9$ [5, part II, p. 73], which reduces to equation (9) when $\mu = 0$. At a similar level of approximation, full plasticity is reached when [5]

$$F = \frac{3\pi a^2 \sigma_y}{\sqrt{1 + \alpha\mu^2}}. \tag{20}$$

The region between these two is the "elastic–plastic" regime; for this, no analysis is at present available. For consistency, we approximate the behaviour in the elastic–plastic regime by modifying equation (11) in the same way to give

$$F = \frac{2}{3}\frac{\pi a^2}{\sqrt{1 + \alpha\mu^2}}\left[2 + \ln\left(\frac{Ea}{3\sigma_y R}\right)\right]\sigma_y. \tag{21}$$

These equations define the boundaries of the regimes of elastic, plastic, elastic–plastic and brittle regimes, in the same way as before. The boundary of the regime at which plasticity first starts is given by

$$\frac{\sigma_y}{E} = \frac{2a}{3\pi R}\frac{\sqrt{1 + \alpha\mu^2}}{(1 - \nu^2)}. \tag{22}$$

The elastic–plastic/fully plastic boundary is unchanged from the static case. The fully plastic/brittle boundary becomes

$$\frac{\sigma_y}{E} = \frac{\sqrt{1 + \alpha\mu^2}}{1.12\left[\frac{1}{2} + \frac{39}{16}\pi\mu\right]}\frac{1}{\sqrt{\pi c}}\left(\frac{J_{1C}}{E}\right)^{1/2}. \tag{23}$$

The elastic/brittle boundary is

$$\frac{J_{1C}}{E} = \left(\frac{1.12}{8\pi}\left[1 + \frac{39}{8}\pi\mu\right]\frac{a}{R}\right)^2 \pi c \tag{24}$$

and the elastic–plastic/brittle boundary is

$$\frac{\sigma_y}{E} = \frac{\sqrt{1 + \alpha\mu^2}}{1.12\left[\frac{1}{9} + \frac{13}{24}\pi\mu\right]\left[2 + \ln\left(\frac{Ea}{3\sigma_y R}\right)\right]}\frac{1}{\sqrt{\pi c}}\left(\frac{J_{1C}}{E}\right)^{1/2}. \tag{25}$$

The boundaries are shown on Fig. 8, which is calculated for $\mu = 0.5$. The solid boundaries, as before, are for values of $a/R = 0.1$ and $c = 10\,\mu$m. The broken lines show how the boundaries shift for other values of a/R and c. The main effect of sliding with friction is to enhance the brittle regime, and to shrink the elastic regime at all their boundaries. The figure suggests that many materials which are elastic or plastic under static indentation become brittle when the indenter slides.

3. SUMMARY AND CONCLUSIONS

The response of a material to load can be elastic, plastic or brittle. At an approximate level, the response depends on two material properties, σ_y/E and J_{1C}/E, and so on the nature of loading. The relevant material response is displayed by a diagram with σ_y/E and J_{1C}/E as axes, shown here on Fig. 3. Materials of a given class cluster together on such a diagram; thus elastomers occupy one area, polymers another, metals a third, ceramics a fourth and so on. The loading defines boundaries on this figure, identifying fields of elastic, brittle, plastic and elastic–plastic response. The sizes of the fields depend on the details of the loading. Three examples are developed here: simple tension, static indentation and indentation with frictional sliding. The diagrams give insight into the way a given material will behave for each type of loading.

In order to pursue the above approach several approximations have been made. The temperature

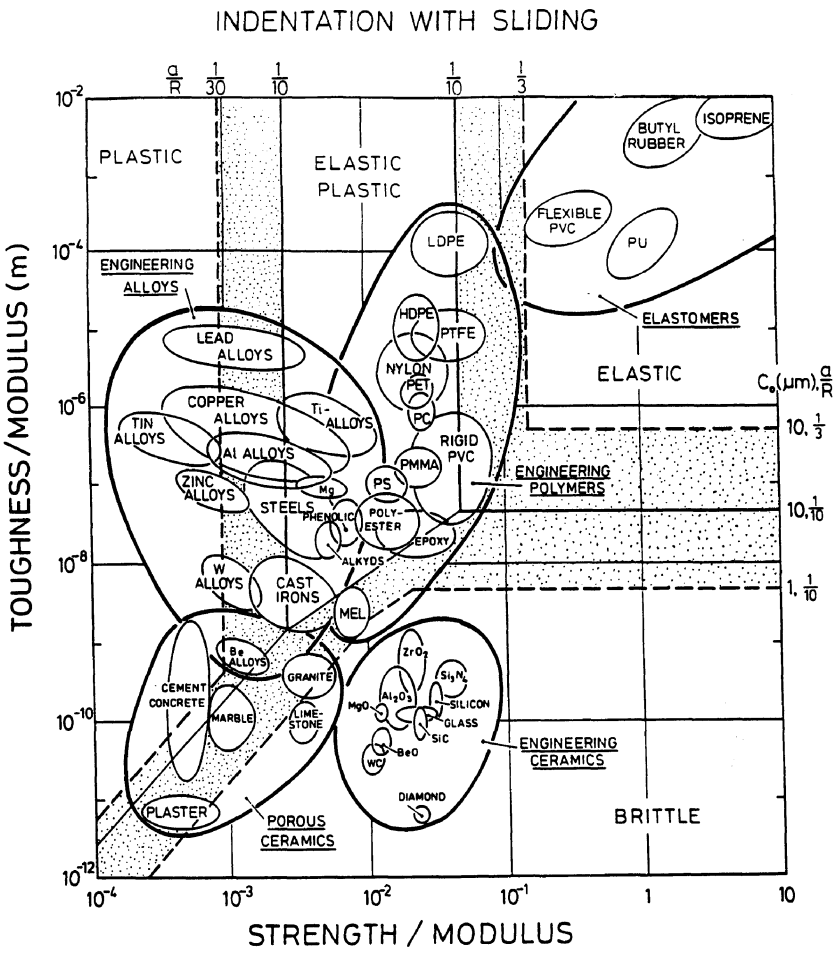

Fig. 8. The chart of Fig. 3, showing the mechanism–transition boundaries for indentation with sliding.

and strain rate dependence of the three properties σ_y, J_{1C} and E have been ignored. To fix the boundaries Poisson's ratio, ν, was taken to be 1/3, a reasonable average value for most materials. In the sliding contact case, at velocities below about 1 m/s frictional heating is negligible, [13] and was ignored. The values of J_{1C} for elastomers were taken to be equal to their tear energies.

The J_{1C}/E against σ_y/E indentation map shows that many materials lie within the coupled elastic–plastic indentation regime, where elastic and plastic strains are comparable. Only a few materials fall into a non-coupled regime, such as lead, copper and tin within the plastic regime; diamond in the brittle regime and elastomers within the elastic regime. The classification of materials under indentation agrees with many observations. These include the classical plasticity experiments performed on copper; plasticity occurring in aluminas, which are traditionally thought of as purely brittle and the lack of cracking in PMMA and epoxies under indentation, despite their brittleness in tension.

Indentation with sliding, enlarges both the brittle and the plastic fields compared with static indentation. Most engineering ceramics now lie in the brittle regime, as compared with the elastic–plastic regime under static indentation. Under sliding contact most metals and their alloys lie in the plastic regime. This appears to be reasonable from experimental evidence, such as scratch tests for ceramics, and friction and wear tests of metals [14]. The elastic–plastic regime is reduced in size, leaving the polymer response to a sliding contact little changed from that of indentation, although, at the elastic–plastic/brittle boundary, brittle polymers such as epoxies and melamines, may show brittle behaviour. Elastomers remain purely elastic in response.

Acknowledgements—We wish to acknowledge many helpful discussions with Professor K. L. Johnson and Dr J. A. Greenwood, and the support of the SERC through a quota award.

REFERENCES

1. K. L. Johnson, *Contact Mechanics*. Cambridge Univ. Press (1985).
2. M. F. Ashby, *Mater. Sci. Technol.* **5**, 517 (1989).
3. M. F. Ashby, *Indian J. Technol.* **28**, 217 (1990).
4. D. Cebon and M. F. Ashby, *Metals Mater.* **8**, 25 (1991).
5. F. P. Bowden and D. Tabor, *The Friction and Lubrication of Solids*, Parts I and II. Oxford Univ. Press, Oxford (1950, 1964).
6. L. E. Samuels and T. O. Mulhearn, *J. Mech. Phys. Solids* **5**, 125 (1956).
7. B. R. Lawn and T. R. Wilshaw, *Fracture of Brittle Solids*. Cambridge Univ. Press, Cambridge (1975).
8. B. R. Lawn, *Proc. R. Soc. Lond. A* **299**, 307 (1967).
9. B. R. Lawn and A. G. Evans, *J. Mater. Sci.* **12**, 2195 (1977).

10. B. R. Lawn, S. M. Wiederhorn and D. E. Roberts, *J. Mater. Sci.* **19,** 2561 (1984).
11. H. Kong and M. F. Ashby, *MRS Bull.*, October, p. 41 (1991).
12. G. M. Hamilton, *Proc. Inst. Mech. Engrs* **197c,** 53 (1983).
13. M. F. Ashby, J. Abulawi and H. S. Kong, *ASME/STLE Tribology Trans.* **34,** 577 (1991).
14. R. D. Arnell, P. B. Davies, J. Halling and T. L. Whomes, *Tribology*. Macmillan, New York (1991).